

Thermal Analyses of Phospholipid Mixtures by Differential Scanning Calorimetry and Effect of Doping with a Bolaform Amphiphile

Ryo Sasaki,[1] Hirotaka Sasaki,[1] Seketsu Fukuzawa,*[1] Jun Kikuchi,[2] Hiroshi Hirota,[2] and Kazuo Tachibana*[1]

[1]Department of Chemistry, School of Science, The University of Tokyo and CREST, Japan Science and Technology Corporation (JST), Hongo, Bunkyo-ku, Tokyo 113-0033

[2]Protein Research Group, RIKEN Genomic Sciences Center and Division of Supramolecular Biology, Yokohama City University, Suehiro-cho, Tsurumi-ku, Yokohama 230-0045

Received July 20, 2006; E-mail: seketsuf@chem.s.u-tokyo.ac.jp

Morphological phases of DMPC/DHPC mixtures have already been investigated by using SANS, SAXS, NMR, and fluorescence-based techniques, as well as *cryo*-TEM, in which the manner of temperature is changed stepwise. We continuously monitored temperature-dependent phase transitions of DMPC/DHPC mixtures by DSC. We observed four significant transitions, two of which (transitions 1 and 4) were newly discovered in our current study. It was shown that bicelles have phase transitions similar to vesicles, and we proposed a phase diagram of DMPC/DHPC mixtures based on a continuous temperature change method. Such a phase diagram, in which transition temperatures are shown clearly, has never been reported to our knowledge. Moreover, we studied the doping effect of a synthetic bolaform amphiphile, which is used to construct stable model membranes, and found that the temperature range of the magnetically aligned state shifted to a higher temperature. This result indicates that doping synthetic phospholipids, which is done to create a thermostable membrane, is useful for stabilizing bicelles, worm-like micelles, or perforated lamellae. Such applications might be relevant to a variety of experiments, including those that utilize DMPC/DHPC mixtures as model membranes or alignment media.

Lipid bilayers are fundamental units of biomembranes, where a variety of indispensable life processes occur. Membranes change their characteristics with respect to their components and in response to certain physical conditions, such as temperature, hydration level, and pressure.[1] In order to understand these phenomena, extensive investigations have been carried out using model membrane systems, of which the major components were phospholipids. Detailed elucidation of the morphology of model membranes can provide basic and important information for biological studies, and this information can in turn be used to design more complex model membrane systems.

Bicelles, which are discoidal lipid–detergent mixtures, are the simplest assemblies that include a bilayered structure. Typical bicelles may be composed of a mixture of 1,2-dimyristoyl-3-*sn*-phosphatidylcholine (DMPC; **1** in Fig. 1) and 1,2-dihexanoyl-3-*sn*-phosphatidylcholine (DHPC; **2** in Fig. 1) with the total lipid concentration ($c = \{w(\mathrm{DMPC}) + w(\mathrm{DHPC})\}/v(\mathrm{solvent})$) between 0.05 and 0.35 g mL^{-1}. These bicelles have been proposed to consist of a circular center comprised of DMPC in a lipid bilayer, surrounded by a rim of DHPC[2] and might be used as appropriate membrane protein reconstitution media for X-ray crystallographic analyses due to the possession of a minimal bilayerd structure.[3,4] They can be classified into two categories by the molar ratio of DMPC to DHPC ($q = [\mathrm{DMPC}]/[\mathrm{DHPC}]$) around ca. 2.[5–7] When the q value is less than ca. 2, these aggregates show isotropic character in magnetic field and are preferable to globular micelles for structural elucidation of membrane proteins by nuclear magnetic resonance (NMR).[8–10]

Above $q =$ ca. 2, such aggregates are used to order the membrane-binding biomolecules due to their magnetically alignable character and thereby obtain residual dipolar couplings to aid in the structural elucidation of biomolecules.[11–13] Some recent studies have indicated that discoidal aggregates are found below the gel to liquid-crystalline transition temperature (T_m) of DMPC (ca. 24 °C),[14] and that above the T_m, they transform into the magnetically alignable assemblies, which are thought to be worm-like micelles, ribbons, or perforated lamellae.[15–21] These temperature-dependent morphological transitions of DMPC/DHPC mixtures have been investigated using small-angle neutron scattering (SANS), small-angle X-ray scattering (SAXS), fluorescence, NMR-based techniques, and *cryo*-transmission electron microscopy (*cryo*-TEM).[15,16,18–22] Such detailed characterizations of phospholipid mixtures can provide basic and important information applicable to biological studies and the design of more complex model membrane systems. However, the phase diagrams based upon these previous results do not cover all of the continuous morphological changes that occur in these mixtures. The incompleteness of these diagrams is due to the fact that they illustrate the results of experiments employing techniques, in which the temperature is changed in a stepwise, rather than a continuous, manner.

Archaebacteria are distinct from prokaryotes and eukaryotes and have been classified as a third independent domain.[23–29]

Published on the web June 13, 2007; doi:10.1246/bcsj.80.1208

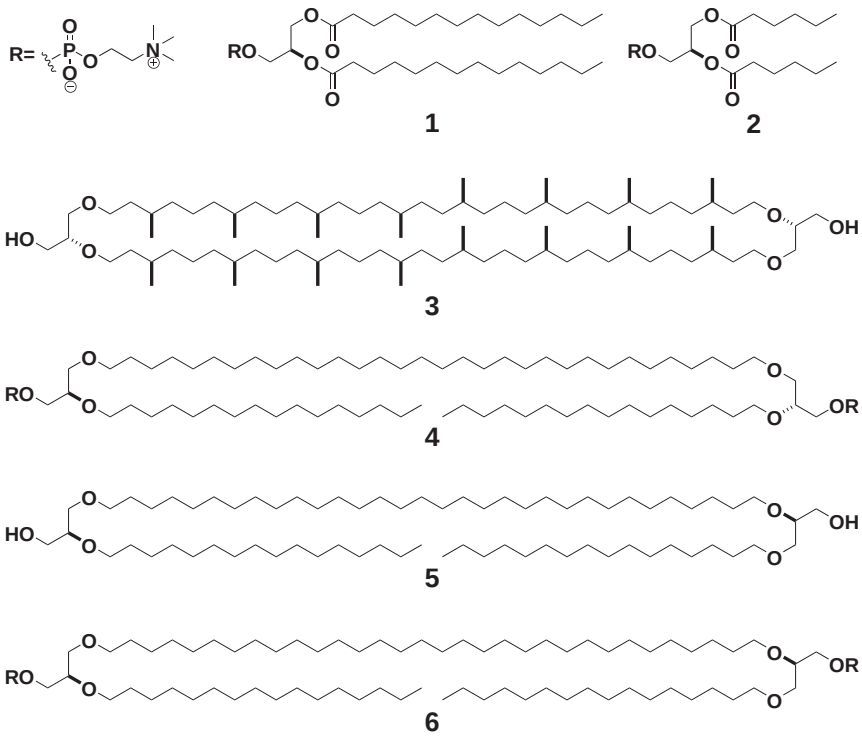

Fig. 1. Structures of various phospholipids.

They usually inhabit extraordinary environments, such as high temperature, highly acidic, and/or salt-rich conditions. The characteristic feature of archaebacteria is found in the chemical structure of the archaeal membrane lipids, which consist of hydrophilic isoprenoid chains linked to glycerol by an ether linkage. Some of these lipids have macrocyclic structures as large as 72-membered rings, such as **3** in Fig. 1; these are known as tetraether lipids.[30–36] These bolaform amphiphiles also constitute an important class of biomimetic materials due to their stability at elevated temperatures, pH extremes, and high ionic strength. Therefore, bolaform amphiphiles are very useful additives for membrane stabilization. Numerous strategies for the synthesis of membrane lipids imitating such bolaform structures have been reported.[37–47] Yamauchi et al. have synthesized the bolaform amphiphile **4**, which formes planar membranes of about 56 Å thickness with a T_m of 61 °C and a ΔH of 16.5 kcal mol^{-1} when prepared appropriately.[37] These parameters indicate the stability of model membranes composed of **4**.

In the present study, we were interested in phase behavior of the DMPC/DHPC mixtures and continuously monitored their temperature-dependent morphological changes using differential scanning calorimetry (DSC).[48–51] Furthermore, we were attracted to the characteristics of archaeal membrane lipids and synthesized the bolaform tetraether phospholipids **5** and **6** using Eguchi's practical methods, and doped DMPC/DHPC bicelles with **6** in order to stabilize them. Our results indicated that four transitions exist in the DMPC/DHPC mixtures, and we determined each transition temperature. Moreover, we characterized the effects of doping with the synthetic bolaform amphiphile, with the aim of constructing stable model membranes using ^{31}P NMR. We found that the temperature range at which a magnetically aligned state was achieved shifted to higher temperatures. These results indicate that bolaform amphiphiles, which form thermostable membrane themselves, confer thermostability to bicelles as well as to vesicles. Such a doping technique is versatile for studying membrane systems.[52,53]

Experimental

General. Analytical TLC was performed using E. Merck silica gel 60 F_{254} plates (0.25 mm thickness). Column chromatography was performed using Kanto Chemical silica gel 60N (40–100 mesh, spherical, neutral). ^{1}H and ^{13}C NMR spectra were recorded on a JEOL JNM-AL-400 or JNM-ECX-400 spectrometer, and chemical shift values are reported in ppm (δ) downfield from tetramethylsilane with reference to internal residual solvent [^{1}H NMR: $CHCl_3$ (7.24), CHD_2OD (3.31); ^{13}C NMR: $CDCl_3$ (77.0), CD_3OD (49.0)]. Coupling constants (J) are reported in hertz (Hz). The following abbreviations are used to designate the multiplicities: s = singlet, d = doublet, t = triplet, m = multiplet, br = broad. Low- and high-resolution mass spectra were recorded on a JEOL JMS-MS-700P mass spectrometer under fast atom bombardment (FAB) conditions using *m*-nitrobenzyl alcohol (NBA) as a matrix.

Materials. DMPC and DHPC were purchased from Sigma Chemical (St. Louis, MO, U.S.A.) or Avanti Polar Lipids (Alabaster, AL, U.S.A.) and were used without further purification. All water used for experiments was obtained from a Milli-Q system (Millipore, Bedford, MA, U.S.A.). Anhydrous *N*,*N*-dimethylformamide (DMF) was purchased from Kanto Chemical and used without further drying. $CHCl_3$ and *N*,*N*-diisopropylethylamine (DIEA) were distilled from calcium hydride under argon. All other reagents were purchased at highest commercial grade and used as supplied unless otherwise noted.

Synthesis of Diol 5. See Ref. 42.

Synthesis of Phosphatidylcholine 6. To a solution of diol **5** (25.6 mg, 0.0237 mmol) in $CHCl_3$ (3 mL) were added DIEA (0.25 mL, 1.43 mmol) and 2-chloro-1,3,2-dioxaphospholane (0.09 mL, 1.01 mmol), and this mixture was stirred at rt for 30 min. TLC indicated that the reaction was not complete, and therefore, additional DIEA (0.125 mL, 0.72 mmol) and 2-chloro-1,3,2-dioxaphospholane (0.045 mL, 0.50 mmol) were added. After 30 min, DIEA (0.065 mL, 0.38 mmol) and 2-chloro-1,3,2-dioxaphospholane (0.022 mL, 0.26 mmol) were added, and then the reaction was continued for additional 30 min. Pyridinium tribromide (808 mg, 2.27 mmol) was added, and the mixture was stirred at rt for 45 min. The mixture was diluted with water (2 mL) and stirred at rt for 2 h. The organic phase was washed with brine and concentrated under reduced pressure. The residue was dissolved in DMF (2 mL), and to this solution was added Me_3N (40% aqueous solution, 6 mL). The reaction mixture was stirred at rt for 4 days, then concentrated under reduced pressure. The residue was purified by column chromatography (silica gel, 30% MeOH/$CHCl_3$ → 6:14:1 → 7:13:1 → 10:10:2 MeOH/$CHCl_3$/aqueous-NH_3) and lyophilized from water to give phosphatidylcholine **6** (8.8 mg, 26%): ^{1}H NMR (400 MHz, CD_3OD–$CDCl_3$ v/v = 1:1) δ 3.96 (br, 4H), 3.60 (br, 4H), 3.31 (br, 11H), 3.16 (br, 5H), 2.92 (s, 18H), 1.26 (br, 8H), 0.97 (br, 108H), 0.59 (t, J = 5.2 Hz, 6H); ^{13}C NMR (100 MHz, CD_3OD–$CDCl_3$ v/v = 1:1) δ 77.6, 77.5, 71.2, 70.1, 70.0, 57.6, 53.5, 31.4, 29.5, 29.18, 29.16, 29.0, 28.9, 25.6, 25.5, 22.1, 13.3; HRMS (FAB) calcd for $C_{80}H_{166}N_2O_{12}P_2$ [$(M + H)^+$] 1410.1994, found 1410.2006.

Preparation of DMPC/DHPC Mixtures. A 749.7 mM stock solution of DHPC was prepared as follows: an appropriate amount of DHPC was dried in vacuo for 6.5 h, weighed, and dissolved in water. An appropriate amount of DMPC was also weighed after drying and suspended with water. Each solution was homogenized by vortexing followed by several freeze (−78 °C)/thaw (50 °C) cycles.[52]

DMPC/DHPC mixtures were prepared by adding the appropriate volume of DHPC stock solution to a DMPC solution just before each experiment. This phospholipid mixture was warmed to 50 °C and homogenized by vigorous vortexing followed by several freeze (−78 °C)/thaw (50 °C) cycles. After being cooled to 0 °C, the phospholipid mixture was vigorously vortexed until the mixture turned transparent.

Preparation of 6-Doped DMPC/DHPC Mixtures. Compound **6**-doped DMPC/DHPC mixtures with a lipid concentration ($\{w(\mathbf{6}) + w(\text{DMPC}) + w(\text{DHPC})\}/v(\text{solvent})$) and q value ($\{[\mathbf{6}] + [\text{DMPC}]\}/[\text{DHPC}]$) of 0.07 g mL^{-1} and 2.0 (molar ratio), respectively, were prepared as follows: **6** and DMPC were mixed, and dispersed in water. This mixture was warmed to 72 °C and homogenized by vortexing, followed by several freeze (−78 °C)/thaw (72 °C) cycles. To this mixture were added DHPC stock solution, water and D_2O. This mixture was cooled to 0 °C and homogenized by vortexing, followed by several freeze (−78 °C) and thaw (72 °C) cycles.

DSC Experiments. DSC experiments were performed with a Bruker AXS DSC3200S (Yokohama, Japan). Samples (50 μL) having different q values ranging from 0.5 to 5.0 in water contents were loaded into gold-coated silver pans and sealed in a cold room, in which the temperature was maintained at 0 °C, because these samples became very viscous at room temperature. Both sample and reference pans were placed in the calorimeter and thermally equilibrated at 0 °C for 1 h. The temperature was scanned from 5 to 60 °C at a heating rate of 1.0 °C min^{-1}. Functional analyses of DSC traces were performed using Bruker AXS WS002 Ver.3.60 and DSCAREA Ver.3.20 operating software. The transition temperature was confirmed by time differentiation of the DSC trace. DSC measurements were carried out three or four times for each sample, and reproducibility of their DSC traces was confirmed.

^{31}P NMR Experiments. ^{31}P NMR was carried out on a JEOL JNM-ECX-400 spectrometer (Akishima, Japan) with a 5 mm tunable multi-nuclear probe. All samples were dissolved with 90% H_2O/10% D_2O. All spectra were collected with both the deuterium field frequency lock, and sample spinning turned off. ^{31}P (161.83 MHz) spectra were acquired using a 90° ^{31}P pulse (10 μs), WALTZ ^{1}H decoupling (^{1}H 90° pulse 115 μs), and a relaxation delay of 2.0 s between scans. Spectra were collected with 32768 points, 128 scans and a sweep width of 70 ppm centered at 0 ppm. A deuterium (D_2O) lock was used, and ^{31}P chemical shifts were referenced to 80% H_3PO_4 (H_3PO_4 = 0 ppm). Samples were allowed to equilibrate at the desired temperature for at least 20 min prior to the acquisition of NMR data.

Results and Discussion

DSC of DMPC/DHPC Mixtures. Figure 2 shows DSC thermograms and the differential curves of DMPC/DHPC mixtures (c = 0.1 g mL^{-1}, q = 0.5, 1.0, 1.5, 1.8, 2.0, 2.5, 3.0, 3.2, 3.8, 4.0, and 5.0, respectively). Below q = 1.0, phase transition was ambiguous. However, above q = 1.5, DSC thermograms were distinguishable. The main transition of DMPC around 24 °C could be clearly observed.[54,55] Another endothermic transition appeared at ca. 20 °C above q = 2.5. The time differentiation curve showed the lowest phase transition (ca. 14 °C) was not endothermic. The most complicated thermal profiles were seen at q values of 2.5, 3.0, and 3.2. In these cases some small endothermic transitions around ca. 48 °C appeared.

Transition Parameters. The series of DSC thermograms of DMPC/DHPC mixtures shown in Fig. 2 indicated that there are four major of transitions (1, 2, 3, and 4 in Fig. 3) defined on the three independent baselines (I, II, and III in Fig. 3). We determined transition temperatures (T_i, T_m, and T_f) as follows: (1) a non-endothermic transition, in which T_i and T_f correspond to onset and completion of the transition, respectively, which intersect points of baseline I and a tangent at the midpoint of the transition (In this case, transition enthalpy does not exist.), (2) an endothermic transition, and (3) T_m, given by the minimum of the endothermic peak of the DSC thermogram, corresponds to the midpoint of the transition.[54] Transition enthalpies (ΔH) were determined from the areas enclosed between the endothermic peaks and the interpolated baselines (area C in Fig. 3). In the case of overlapping peaks, a graphical evaluation was adopted (areas A and B in Fig. 3). In addition, in the case of the peak, of which the baseline on the low temperature side differed from that on the high-temperature side, area B was determined as the sum of areas B_1 and B_2 in Fig. 3 by using Sturtevant's method.[54] All transition parameters are summarized in Tables 1 and 2.

Figure 4 shows enthalpy plots for different q values of DMPC/DHPC mixtures at the transitions 2, 3, and 4 (these correspond to ΔH_2, ΔH_3, and ΔH_4, respectively). Transition 2 was observed under the condition of $q > 2.0$, and the ΔH_2 value increased in proportion to the q value, except when q = 4.0. Transition 3 was observed in all samples except in

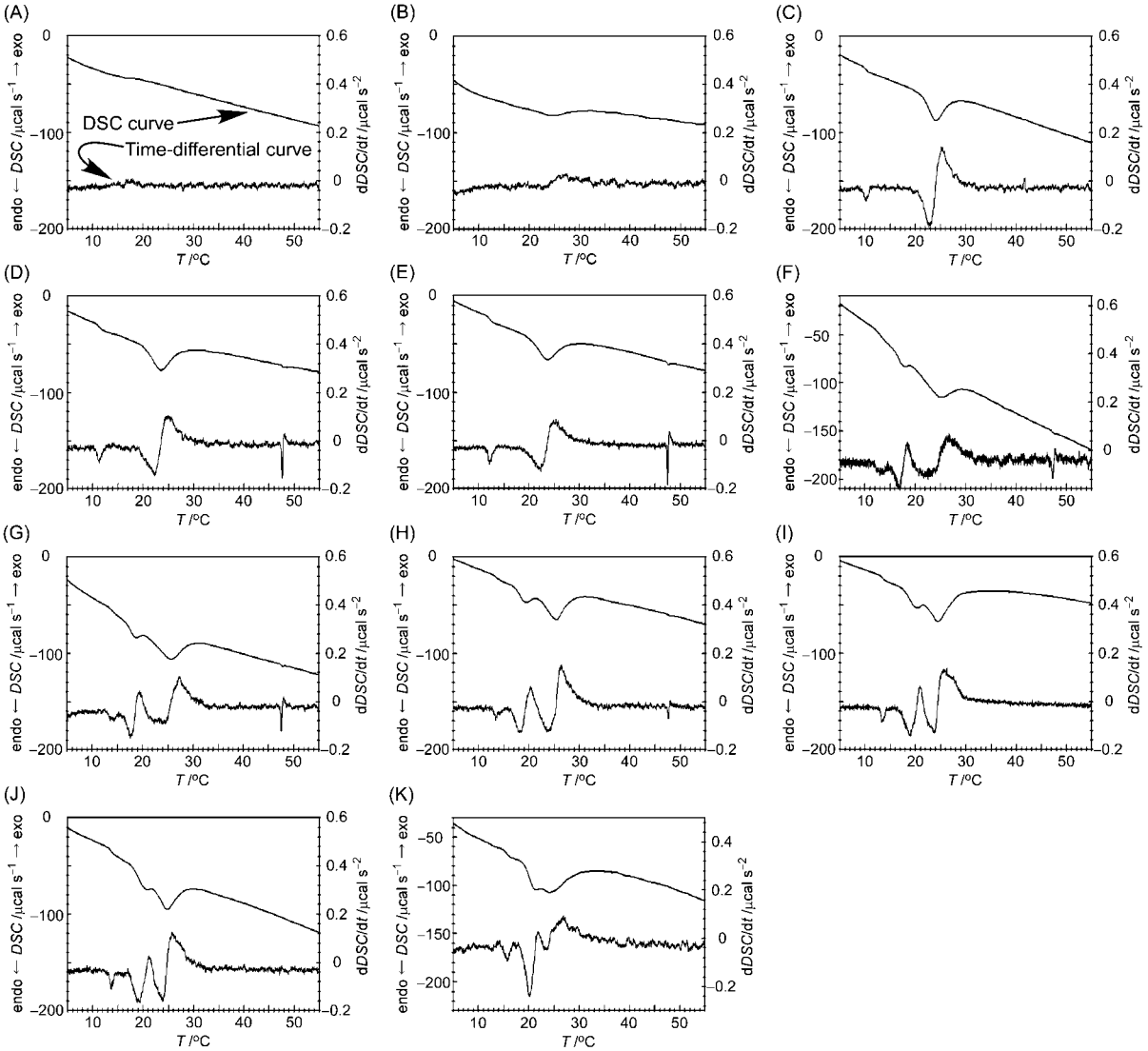

Fig. 2. DSC thermograms of DMPC/DHPC mixtures ($c = 0.1\,\mathrm{g\,mL^{-1}}$; $q = 0.5$ (A), 1.0 (B), 1.5 (C), 1.8 (D), 2.0 (E), 2.5 (F), 3.0 (G), 3.2 (H), 3.8 (I), 4.0 (J), and 5.0 (K)). Heating rate was $1.0\,^{\circ}\mathrm{C\,min^{-1}}$.

the case of $q = 0.5$ and gave the largest enthalpy value among the three kinds of endothermic transitions. Transition 4 at $1.5 < q < 3.8$ gave the smallest value of enthalpy among the three kinds of endothermic transitions.

Morphological Changes of DMPC/DHPC Mixtures. Phases and phase transitions of phosphatidylcholines have been well studied.[55,56] For DMPC multilamellar vesicles, the pretransition and the main transition temperatures have been reported to be 11.4 ± 4.9 and $23.6 \pm 1.5\,^{\circ}\mathrm{C}$, respectivily.[55] Generally, the interpretation of phase behavior of binary mixture of phospholipids is difficult.[56] Although no major endothermic transition was observed under the condition of $q = 0.5$, an endothermic transition at $24\,^{\circ}\mathrm{C}$ (transition 3) appeared at $q = 1.0$ in our results. Above the $q = 1.5$, the phase transitions were observed more clearly, and the thermograms were understandable, because they were consistent with the non-endothermic transition (transition 1) as well as a main transition (transition 3). Koynova et al. have reported that transition 2, observed at $q > 2.5$, is the pre-transition of the DMPC bilayer.[56] This transition temperature increased concomitantly with increases in the q value. Transition enthalpy ΔH_2 also increased dependent on the q value, except when $q = 4.0$. This upward trend in the value of transition temperature and enthalpy indicated that an increase of the q value made the size of bilayered planes of bicelles larger and that resulted in stabilizing DMPC bilayer was more stable. Transition 3, which is the main transition of the DMPC bilayer, began upon completion of transition 2. Finally, transition 4, observed at ca. $47\,^{\circ}\mathrm{C}$ and $1.5 < q < 3.8$, was the smallest of all endothermic transitions observed.

To assist the interpretation of the morphological changes of DMPC/DHPC mixtures we measured $^{31}\mathrm{P}$ NMR spectra at $q = 2.0$ (Fig. 5). $^{31}\mathrm{P}$ resonance gives rise to a signal, of which the chemical shift, linewidth, and lineshape are indicative of the phospholipid phase state or of local order around the head group and/or polymorphism.[1] At $10\,^{\circ}\mathrm{C}$, DMPC/DHPC mixtures composed of 10% (w/v) total lipids have been reported to form bicelles,[18] and a couple of narrow (17-Hz width at half-height) and broad (87-Hz width at half-height) isotropic peaks were observed at 2.4 and 2.2 ppm, respectively. The nar-

Table 1. Transition Temperatures of DMPC/DHPC Mixtures

q	DMPC /mol %	T_{i1} /°C	T_{f1} /°C	T_{i2} /°C	T_{m2} /°C	T_{f2} /°C	T_{i3} /°C	T_{m3} /°C	T_{f3} /°C	T_{i4} /°C	T_{m4} /°C	T_{f4} /°C
0.5	33							13.1	19.9			
1.0	50	15.4	17.1					24.4	29.5			
1.5	60	9.7	10.9				21.4	24.1	27.7			
1.8	64	10.9	12.2				20.0	23.6	28.8	47.6	48.0	48.7
2.0	67	11.7	12.8				20.0	23.6	28.4	47.3	47.7	48.4
2.5	71	12.3	13.9	15.6	18.0	19.6	18.6	25.3	29.2	47.0	47.6	48.4
3.0	75	13.1	14.9	16.6	18.8	20.8	20.0	25.6	29.4	47.4	47.7	48.3
3.2	76	12.6	14.6	16.7	19.2	21.7	21.3	25.3	28.9	47.4	47.8	48.6
3.8	79	13.4	14.5	17.7	20.5	23.3	20.9	24.5	28.5			
4.0	80	13.2	13.9	17.9	20.8	22.7	21.1	24.8	28.6			
5.0	83	14.9	16.0	19.2	21.6	23.6	22.2	24.3	30.7			

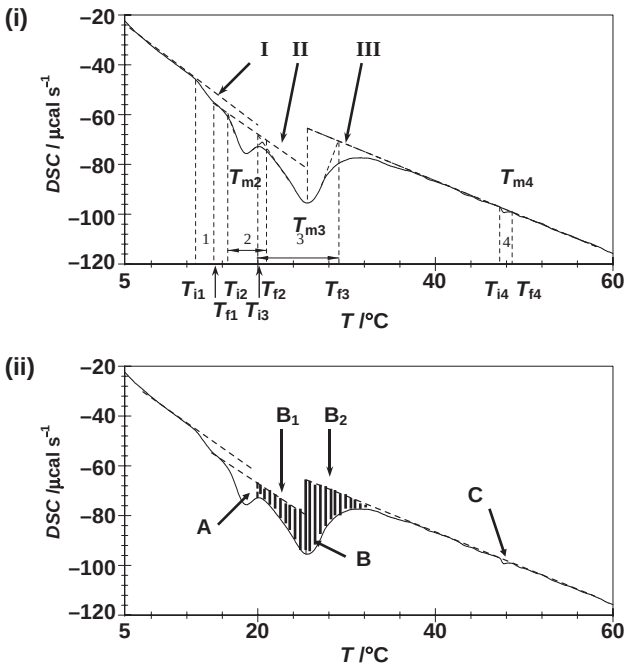

Fig. 3. Determination of transition temperatures (i) and enthalpies (ii) of DMPC/DHPC mixtures.

Table 2. Transition Enthalpies of DMPC/DHPC Mixtures

q	DMPC /%	ΔH_2 /cal mol^{-1}	ΔH_3 /cal mol^{-1}	ΔH_4 /cal mol^{-1}
0.5	33.3			
1.0	50.0			
1.5	60.0		1322	
1.8	64.3		1635	17.6
2.0	66.7		1440	17.7
2.5	71.4	204	975	16.3
3.0	75.0	290	1208	10.2
3.2	76.2	374	1332	6.20
3.8	79.2	441	1218	
4.0	80.0	407	1233	
5.0	83.3	716	2721	

row peak reflects the higher mobility of phospholipids molecules and was assigned to DHPC at the rim region of bicelles. The broad peak seemed to be derived from a less mobile gel-phase DMPC at the planar region of bicelles. At 15 °C, ^{31}P NMR profile slightly changed; a couple of narrow (35-Hz width at half-height) and broad (43-Hz width at half-height) isotropic peaks were observed at 2.4 and 2.2 ppm, respectively. Transition 1 is some specific arrangement of phospholipid molecules. ^{31}P NMR spectrum at 25 °C revealed different signals from those below 20 °C: the broad isotropic component was more broadened (668-Hz width at half-height at 2.7 ppm), and a narrow peak (43-Hz width at half-height at 2.5 ppm) appeared. These results imply that the mobility of DMPC/DHPC aggregates was dramatically increased after the transition 3 (23.6 °C) which is the gel-to-liquid-crystalline phase transition of DMPC. Furthermore, the broad component became broader (919-Hz width at half-height) and shifted to 0.7 ppm at 30 °C. This change in the broad peak reflects the transition state from bicelles into perforated lamellae. SANS studies have shown that bicelles and perforated lamellae coexist at 25 °C,[18] and the viscosity of DMPC–DHPC mixtures increases at temperatures between ca. 25 and ca. 30 °C.[57] This result implies that bicelle formation and simultaneous fusion to form perforated lamellae occur around this temperature. Therefore, the broad component in both ^{31}P NMR spectra at 25 and 30 °C seemed to be derived from the liquid-crystalline-phase DMPC in the bicelles. The narrow one was from DHPC at the rim region and in micelles. Aggregates composed of larger amounts of phospholipids have a greater tendency to align in a magnetic field.[58] Thus, the up field shift of the broad component in the ^{31}P NMR spectrum at 30 °C also supports the enlargement of bicelles. SANS and NMR-based tracer self-diffusion studies have shown that perforated lamellae form at 35 °C.[17,18,20,21] Two anisotropic peaks (1.1 ppm with half-height width of 43 Hz for DHPC, and −3.3 ppm with half-height width of 381 Hz for DMPC) that indicated the formation of perforated lamellae were observed in the ^{31}P NMR spectrum at this temperature. One might think that the NMR signals from phospholipids lamellae should be quite broad because of their huge aggregate size. However, once perforated lamellae formed, the NMR peaks from both of DHPC and DMPC became relatively sharp regardless of their large assembly sizes. This phenomenon seems to be derived from the fast lateral movement of DHPC pores, which induces the movement of DMPC in perforated lamellae. Typical perforated-lamellar-associated peaks were also observed between 40 and 45 °C,

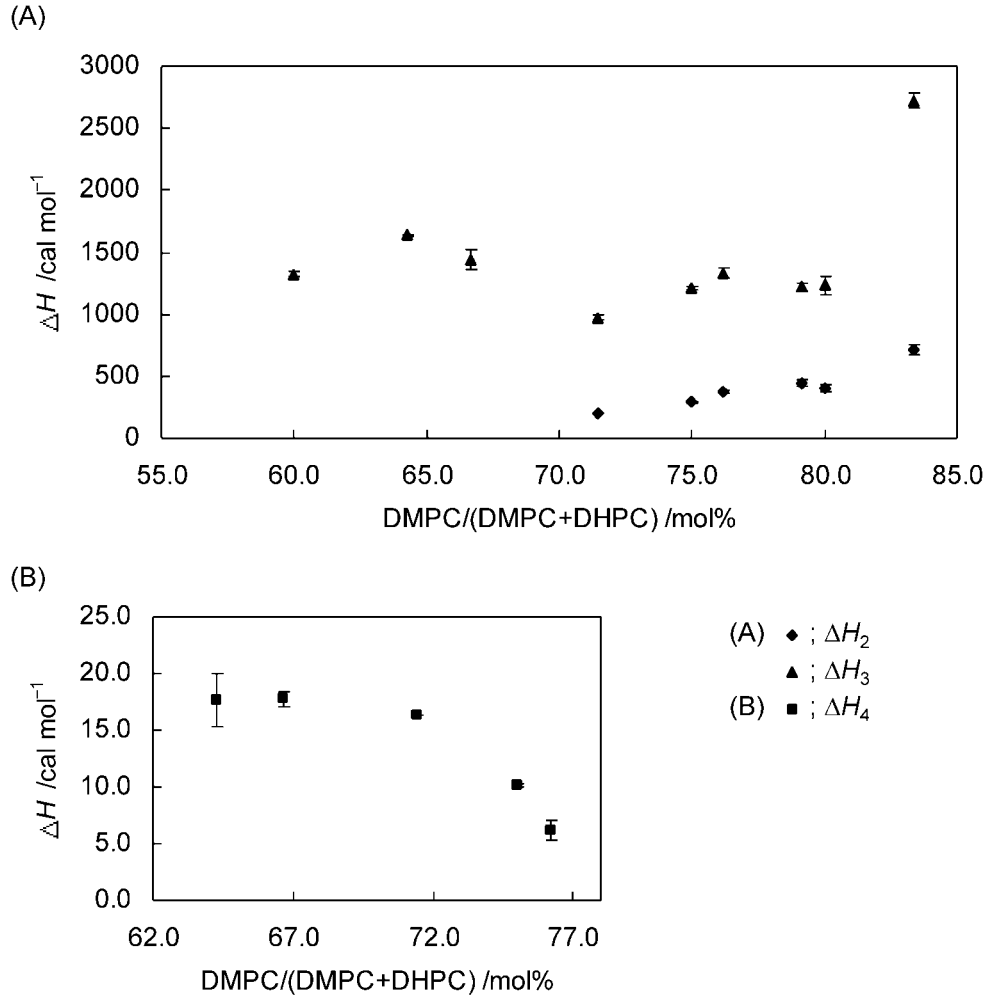

Fig. 4. Plots showing the transition enthalpies of DMPC/DHPC mixtures; (A) closed diamond points (◆) and closed triangle points (▲) indicate the enthalpies at transition 2 (ΔH_2) and at transition 3 (ΔH_3) respectively. (B) Closed square points (■) indicate the enthalpies at transition 4 (ΔH_4).

and each of their half-height widths remained almost unchanged (35 and 191 Hz). However, both of these peaks shifted up field compared with those at 35 °C. This result implies that some rearrangement, other than fusion, of perforated lamellae into a highly oriented state occurs. SANS studies have shown that perforated lamellae in cuvettes are composed of two orientationally distinct lamellar domains, of which the interfaces are seemingly populated with defects lying on a 2D centered rectangular lattice.[19] Therefore, the chemical shifts of anisotropic peaks in ^{31}P NMR spectra indicate an averaged alignment of these two lamellar domains. At 50 °C, the two anisotropic peaks indicative of perforated-lamellar formation completely disappeared, and a couple of narrow (26-Hz width at half-height) and broad (234-Hz width at half-height) peaks appeared at 2.7 and −10.6 ppm, respectively. Judging from its broadness and chemical shift, the NMR peak at −10.6 ppm seems to be due to a huge magnetically aligned assembly. Moreover, the narrow peak at 2.7 ppm implies that isotropically tumbling small aggregates formed. These results suggest a unique disruption model of perforated lamellae after the transition 4 (47.7 °C), that is, DHPC pores are blown out and perforated lamellae are transformed into DMPC lamellae. The broadness of the NMR peak at −10.6 ppm (234 Hz width at half-height) is reasonable for lamellar size, and up field shift of the DMPC peak from that of perforated lamellae seems to be caused by the elimination of intersecting perforated lamellae and the formation of uniformly aligning lamellae.

According to results of previous investigations,[5] DMPC/DHPC mixtures had the ability to magnetically align above 24 °C, and therefore, the progression from discoidal aggregates to this state (worm-like micelles, ribbons, or perforated lamellae)[15,16] could be observed as a broad endothermic peak in DSC thermograms. Transition enthalpy ΔH_3 was not dependent on the q value. We think that the ΔH_3 value is related to existence of transition 2 and/or transition 4 as follows: (i) when both transitions 2 and 4 existed ($2.5 \leq q \leq 3.2$), the ΔH_3 value increased dependent the q values, and (ii) when only transition 4 existed ($1.8 \leq q \leq 2.5$), the ΔH_3 value decreased, which indicated that enlargement of the size of bilayerd plane was possibly concomitant with the relaxation of molecular packing around the hydrophobic lipid assemblies of the bilayerd plane. Finally, transition 4, observed at ca. 47 °C and $1.5 < q < 3.8$, was the smallest of all endothermic transitions observed, which indicated that this transition corresponded not

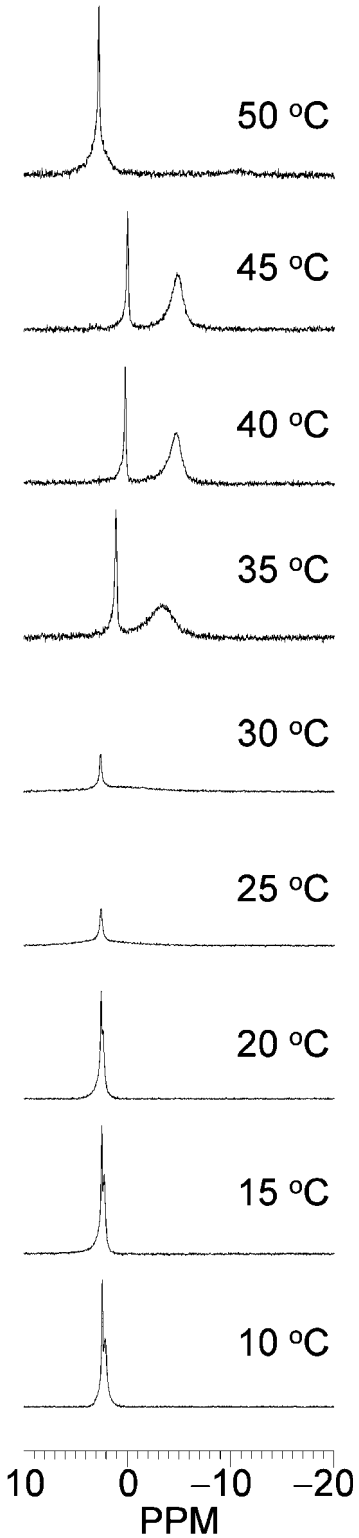

Fig. 5. ^{31}P NMR spectra of DMPC/DHPC mixture (c = 0.1 g mL^{-1}, [DMPC]/[DHPC] = 2.0, ppm from ext. H_3PO_4 = 0 ppm.

to changes in the DMPC side chains, but to a morphological change. ^{31}P NMR experiments indicated that the magnetic alignment had collapsed around this temperature (Fig. 5). Transition enthalpy ΔH_4 decreased concomitantly with an increase in the q value and was not observed, except in the specific range of $1.5 < q < 3.8$. The q value around this range correspond to the magnetically aligning character of DMPC/DHPC mixtures, and therefore, transition 4 is significant for understanding the magnetically aligned character. A phase diagram for DMPC/DHPC mixtures, constructed from the temperatures of onset and completion of the excess heat capacity changes in DSC scans, is given in Fig. 6.[59] Dashed lines are reported from NMR experiments previously, and the solid lines are current result.

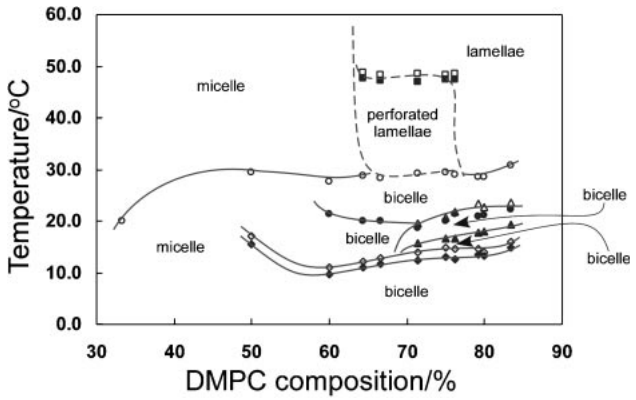

Fig. 6. Phase diagram of DMPC/DHPC mixtures (c = 0.1 g mL^{-1}). Closed diamonds (◆), closed squares (■), closed triangles (▲), open triangles (△), and asterisks (∗) correspond to the onset temperatures of transition 1 (T_{i1}), the completion temperatures of transition 1 (T_{f1}), the middle temperature of transition 2 (T_{m2}), the middle temperature of transition 3 (T_{m3}), and the middle temperature of transition 4 (T_{m4}), respectively.

Effect of Doping DMPC/DHPC Mixtures with Bolaform Tetraether Phospholipid 6. Addition of bolaform amphiphile **6** induced a higher temperature shift in the magnetic alignment of the DMPC/DHPC aggregates (Fig. 7, c = 0.07 g mL^{-1}, q = {[**6**] + [DMPC]}/[DHPC] = 2.0, and r (molar ratio of additive) = [**6**]/{[**6**] + [DMPC]} = 0.05 (A), 0.1 (B), 0.2 (C), 0.9 (D)), and the special features were dose dependent. For example, in Fig. 7B, when r = 0.1, a sharp signal at 2.5 ppm (half-height width of 43 Hz) was observed, indicating that the aggregates were not magnetically aligned at 30 °C. At 35 °C a spectrum indicating magnetic alignment of the aggregates was observed. The spectral profile at 50 °C indicated magnetic alignment, although it differed from that obtained by doping free DMPC/DHPC mixtures. This magnetic alignment collapsed at 60 °C. A higher dose of **6** (r = 0.2) resulted in signal broading of ^{31}P NMR spectra above 45 °C as shown in Fig. 7C, which indicated that fluidity of phospholipid aggregates decreased. DMPC/DHPC mixtures are known to align in a magnetic field at 30–45 °C (Fig. 5).[12] This magnetically alignment feature was detected by down field and up field signals corresponding to DHPC and DMPC. Doping DMPC/DHPC mixtures with bolaform tetraether phospholipid **6** (r = 10 mol %) caused the magnet alignment temperature to shift to a higher value (Fig. 7). This indicates that addition of **6** compresses transitions of DMPC/DHPC aggregates by decreasing the fluidity of the lipid-bilayer due to relatively high gel-to-liquid crystalline transition temperature of **6** (64.5 °C). This phenomenon is commonly observed in binary mixtures

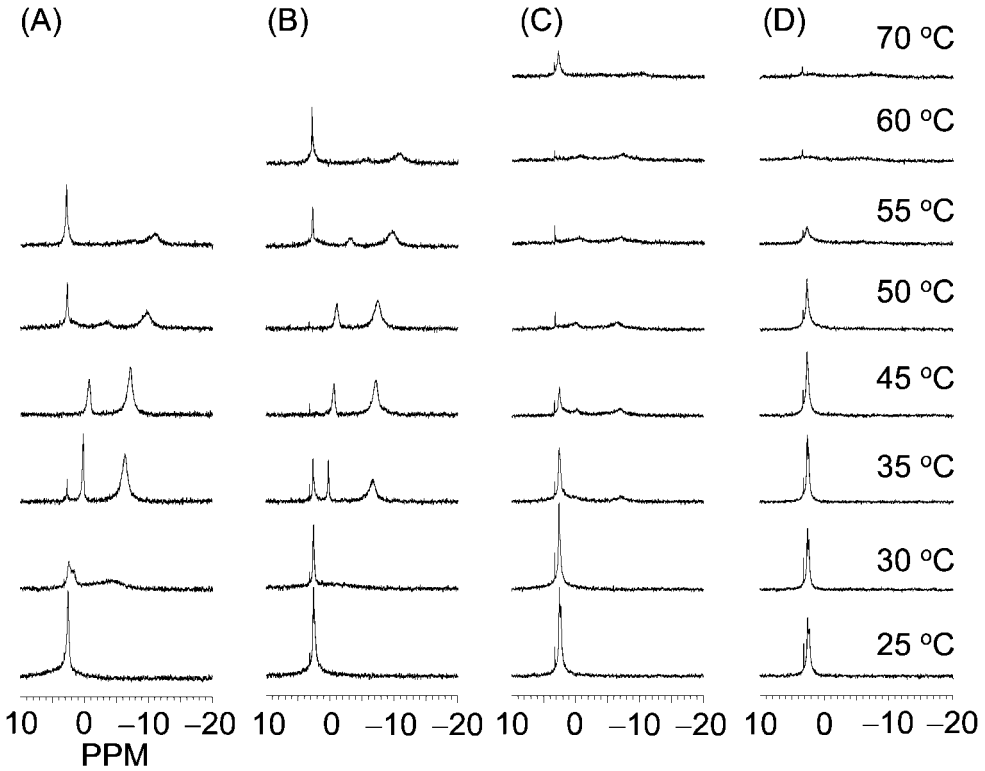

Fig. 7. ^{31}P NMR spectra of **6**/DMPC/DHPC mixtures ($c = 0.07\,\mathrm{g\,mL^{-1}}$, {[**6**] + [DMPC]}/[DHPC] = 2.0, [**6**]/{[**6**] + [DMPC]} = 0.05 (A), 0.1 (B), 0.2 (C), 0.9 (D)). ppm from ext. $H_3PO_4 = 0$ ppm.

of phospholipids, and our results are consistent with this interpretation. The types of morphological changes seen in DMPC/DHPC aggregates are also strongly affected by the main transition (gel-to-liquid crystalline transition) of the lipid bilayer, and thus, the transition temperatures can be increased by doping with additives having higher main transition temperatures.

Conclusion

Morphological phases of DMPC/DHPC mixtures have been investigated previously by SANS, SAXS, NMR, fluorescence-based techniques, and *cryo*-TEM, in conjunction with stepwise changes in temperature. We monitored temperature-dependent phase transitions of DMPC/DHPC mixtures that occur during continuous changes in temperature by DSC. Our results showed that there were four significant transitions, and two of them (transitions 1 and 4) were newly discovered in our current study. It is apparent that bicelles have lipid-bilayer transitions, which are similar to those of vesicles, and we constructed a phase diagram of DMPC/DHPC mixtures on the basis of our results obtained using continuous temperature changes. DMPC/DHPC mixtures are popular phospholipid mixtures for model membranes or alignable media; therefore, we hope our thermal data is useful for further studies on biological or material sciences. Additionally, we discovered that the temperature ranges, in which DMPC/DHPC aggregates align in a magnetic field, shifted upward after the mixtures were doped with a bolaform tetraether phospholipid. This result indicates that doping with a synthetic phospholipid that forms a thermostable membrane is useful for stabilizing bicelles, worm-like micelles, or perforated lamellae. These results should be applicable to a variety of experiments, including development of methods that utilize DMPC/DHPC mixtures as model membranes or alignment media.

This work was partly supported by a Grant-in-Aid for Scientific Research (No. A16201044) and a Grant-in-Aid for The 21st Century COE Program for Frontiers in Fundamental Chemistry from the Ministry of Education, Culture, Sports, Science and Technology of Japan. Thanks are also due to Dr. Haruhiko Fuwa and Chihiro Tsukano of the University of Tokyo for their technical advice regarding organic syntheses.

References

1 P. R. Cullis, B. Kruijff, *Biochim. Biophys. Acta* **1979**, *559*, 399.
2 J. Bian, M. F. Roberts, *Biochemistry* **1990**, *29*, 7928.
3 S. Faham, J. U. Bowie, *J. Mol. Biol.* **2002**, *316*, 1.
4 M. Caffrey, *J. Struct. Biol.* **2003**, *142*, 108.
5 C. R. Sanders, J. P. Schwonek, *Biochemistry* **1992**, *31*, 8898.
6 R. R. Vold, R. S. Prosser, *J. Magn. Reson., Ser. B* **1996**, *113*, 267.
7 C. R. Sanders, R. S. Prosser, *Ways Means* **1998**, *6*, 1227.
8 R. R. Vold, R. S. Prosser, A. J. Deese, *J. Biomol. NMR* **1997**, *9*, 329.
9 C. R. Sanders, K. Oxenoid, *Biochim. Biophys. Acta* **2000**, *1508*, 129.
10 J. A. Whiles, R. Deems, R. R. Vold, E. A. Dennis, *Bioorg. Chem.* **2002**, *30*, 431.
11 N. Tjandra, A. Bax, *Science* **1997**, *278*, 1111.

12 J. H. Prestegard, A. I. Kishore, *Curr. Opin. Chem. Biol.* **2001**, *5*, 584.
13 A. Bax, *Protein Sci.* **2003**, *12*, 1.
14 A. Blume, *Biochemistry* **1983**, *22*, 5436.
15 L. van Dam, G. Karlsson, K. Edwards, *Biochim. Biophys. Acta* **2004**, *1664*, 241.
16 M.-P. Nieh, V. A. Raghunathan, C. J. Glinka, T. A. Harroun, G. Pabst, J. Katsaras, *Langmuir* **2004**, *20*, 7893.
17 M.-P. Nieh, C. J. Glinka, S. Krueger, R. S. Prosser, J. Katsaras, *Langmuir* **2001**, *17*, 2629.
18 M.-P. Nieh, C. J. Glinka, S. Krueger, R. S. Prosser, J. Katsaras, *Biophys. J.* **2002**, *82*, 2487.
19 M.-P. Nieh, V. A. Raghunathan, H. Wang, J. Katsaras, *Langmuir* **2003**, *19*, 6936.
20 S. Gaemers, A. Bax, *J. Am. Chem. Soc.* **2001**, *123*, 12343.
21 H. Wang, M.-P. Nieh, E. K. Hobbie, C. J. Glinka, J. Katsaras, *Phys. Rev. E* **2003**, *67*, 060902.
22 J. Bolze, T. Fujisawa, T. Nagao, K. Norisada, H. Saito, A. Naito, *Chem. Phys. Lett.* **2000**, *329*, 215.
23 C. R. Woese, G. E. Fox, *Proc. Natl. Acad. Sci. U.S.A.* **1977**, *74*, 5088.
24 C. R. Woese, O. Kandler, M. L. Wheelis, *Proc. Natl. Acad. Sci. U.S.A.* **1990**, *87*, 4576.
25 F. Delong, *Proc. Natl. Acad. Sci. U.S.A.* **1992**, *89*, 5685.
26 J. Kjims, N. Larsen, J. Z. Dalgaard, R. A. Garrett, K. O. Stetter, *Syst. Appl. Microbiol.* **1992**, *15*, 203.
27 L. N. Benachenhou, P. Forterre, B. Labedan, *J. Mol. Evol.* **1993**, *36*, 335.
28 H. P. Klenk, C. Schleper, V. Schwass, R. Brudler, *Biochim. Biophys. Acta* **1993**, *1174*, 95.
29 S. M. Barns, R. E. Fundyga, M. W. Jeffries, N. R. Pace, *Proc. Natl. Acad. Sci. U.S.A.* **1994**, *91*, 1609.
30 M. Kates, C. N. Joo, B. Palameta, T. Shier, *Biochemistry* **1967**, *6*, 3329.
31 C. N. Joo, T. Shier, M. Kates, *J. Lipid Res.* **1968**, *9*, 782.
32 M. D. Rosa, A. Gambacorta, L. Minale, *J. Chem. Soc., Chem. Commun.* **1974**, 543.
33 K. J. Mayberry-Carson, T. A. Langworthy, W. R. Mayberry, P. F. Smith, *Biochim. Biophys. Acta* **1974**, *360*, 217.
34 M. De Rosa, A. Gambacorta, J. D. Bu'Lock, *Phytochemistry* **1976**, *15*, 143.
35 T. A. Langworthy, *Biochim. Biophys. Acta* **1977**, *487*, 37.
36 M. Kate, *The Biochemistry of Archaea (Archaebacteria)*, ed. by M. Kates, D. J. Kushner, A. T. Matheson, Elsevier Press, Amsterdam, **1993**, pp. 261–295.
37 K. Yamauchi, A. Moriya, M. Kinoshita, *Biochim. Biophys. Acta* **1989**, *1003*, 151.
38 K. Yamauchi, Y. Sakamoto, A. Moriya, K. Yamada, T. Hosokawa, T. Higuchi, M. Kinoshita, *J. Am. Chem. Soc.* **1990**, *112*, 3188.
39 J.-M. Kim, D. H. Thompson, *Langmuir* **1992**, *8*, 637.
40 F. M. Menger, X. Y. Chen, *Tetrahedron Lett.* **1996**, *37*, 323.
41 F. M. Menger, Y.-L. Wong, *J. Org. Chem.* **1996**, *61*, 7382.
42 T. Eguchi, H. Kano, K. Arakawa, K. Kakinuma, *Bull. Chem. Soc. Jpn.* **1997**, *70*, 2545.
43 K. Arakawa, H. Kano, T. Eguchi, Y. Nishiyama, K. Kakinuma, *Bull. Chem. Soc. Jpn.* **1999**, *72*, 1575.
44 T. Eguchi, K. Arakawa, K. Kakinuma, G. Rapp, S. Ghosh, Y. Kakatani, G. Ourisson, *Chem. Eur. J.* **2000**, *6*, 3351.
45 A. P. Patwardhan, D. H. Thompson, *Langmuir* **2000**, *16*, 10340.
46 K. Miyawaki, R. Goto, M. Shibakami, *Synlett* **2002**, 1326.
47 K. Miyawaki, R. Goto, M. Shibakami, *Chem. Lett.* **2003**, *32*, 1170.
48 H. Xu, C. Huang, *Biochemistry* **1987**, *26*, 1036.
49 H. Xu, F. A. Stephenson, C. Huang, *Biochemistry* **1987**, *26*, 5448.
50 J. T. Mason, *Biochemistry* **1988**, *27*, 4421.
51 S. Ali, H. Lin, R. Bittman, C. Huang, *Biochemistry* **1989**, *28*, 522.
52 H. Sasaki, S. Fukuzawa, J. Kikuchi, S. Yokoyama, H. Hirota, K. Tachibana, *Langmuir* **2003**, *19*, 9841.
53 H. Sasaki, M. Araki, S. Fukuzawa, K. Tachibana, *Bioorg. Med. Chem. Lett.* **2003**, *13*, 3583.
54 S. Kitamura, J. M. Sturtevant, *Biochemistry* **1989**, *28*, 3788.
55 R. Koynova, M. Caffrey, *Biochim. Biophys. Acta* **1998**, *1376*, 91.
56 R. Koynova, B. Tenchov, G. Rapp, *Chem. Phys. Lipids* **1997**, *88*, 45.
57 J. Struppe, R. R. Vold, *J. Magn. Reson.* **1998**, *135*, 541.
58 F. Picard, M. J. Paquet, J. Levesque, A. Bélanger, M. Auger, *Biophys. J.* **1999**, *77*, 888.
59 T. Heimburg, U. Würz, D. Marsh, *Biophys. J.* **1992**, *63*, 1369.